

## Supporting information

### **A polyaniline-based ECL cytosensor for sensitive detection of circulating tumor cells**

Yongqi Zhang, Tiantong Wu, Chen Yan, Meixing Li\*, Qingming Shen\*

*State Key Laboratory of Flexible Electronics (LoFE) & Jiangsu Key Laboratory for Biosensors, Institute of Advanced Materials (IAM), Nanjing University of Posts & Telecommunications, Nanjing 210023, China.*

\* Corresponding author:

E-mail: iammxli@njupt.edu.cn (M. Li); iamqmshen@njupt.edu.cn (Q. Shen)

#### **Table of contents:**

1. Chemicals and reagents .....	S-2
2. Synthesis of Au NPs .....	S-3
3. Cell culture .....	S-3
4. Cell number and capture efficiency .....	S-3
5. Optimization of the cytosensor.....	S-4
6. Detection performance evaluation.....	S-4
7. Comparison of different methods for CTCs detection .....	S-5

## 1. Chemicals and reagents

The sequences of DNA strands in this study, shown in Table S1, were purchased from Sangon Biotech (Shanghai) Co., Ltd. Human serum was collected from Affiliated Hospital of Nantong University (Nantong, China). Other reagents in this work are all commercially available. Chloroauric acid ( $\text{HAuCl}_4 \cdot 3\text{H}_2\text{O}$ ) and dimethyl sulfoxide (DMSO) were purchased from Sinopharm Chemical Reagent Co., Ltd. Sodium citrate ( $\text{C}_6\text{H}_5\text{O}_7\text{Na}_3$ ), mercaptosuccinic acid (MSA), tripropylamine (TPrA), bis(2',2'-bipyridine)-4'-methyl-4-carboxybipyridine-ruthenium N-succinimidyl ester-bis-(hexafluorophosphate)  $[\text{Ru}(\text{bpy})_2(\text{mcbpy-O-Su-ester})(\text{PF}_6)_2]$  and streptavidin (SA) were purchased from Aladdin Reagents, Inc. Tris (2-carboxyethyl) phosphine hydrochloride (TCEP), Triton X-100, aniline and bovine serum albumin (BSA) were provided by Sigma–Aldrich. 4% paraformaldehyde fixed solution (PFA), Calcein acetoxymethyl ester (Calcein AM), and uranyl acetate were obtained from Jiangsu Keygen Biotech Co., Ltd. Ultrapure water was purified by the Milli-Q system with a resistivity of 18.2  $\text{M}\Omega \cdot \text{cm}$ . Phosphate buffer solution (PBS) was prepared from disodium hydrogen phosphate ( $\text{Na}_2\text{HPO}_4$ ) and sodium dihydrogen phosphate ( $\text{NaH}_2\text{PO}_4$ ) with the addition of 0.1 M potassium chloride (KCl), and the pH value was adjusted to 7.4.

**Table S1.** DNA sequences used in sensing strategies

Name	Sequences (5' →3' )
SYL3C	SH-TTT CAC TAC AGA GGT TGC GTC TGT CCC ACG TTG TCA TGG GGG GTT GGC CTG
MUC1 aptamer (M1)	AGT CTA GGA TTC GGC GTG GGT TAA GCA GTT GAT CCT TTG GAT ACC CTG G
H1	biotin-TTA ACC CAC GCC GAA TCC TAG ACT CAA AGT AGT CTA GGA TTC GGC GTG
H2	AGT CTA GGA TTC GGC GTG GGT TAA CAC GCC GAA TCC TAG ACT ACT TTG-biotin

## 2. Synthesis of Au NPs

515  $\mu\text{L}$  of  $\text{HAuCl}_4$  solution (2% wt) and 99.485 mL of water were mixed in a flask. Then, 588  $\mu\text{L}$  of sodium citrate solution (0.2 M) was added quickly and stirred violently for 5 min, and kept boiling for 30 min until the solution turned wine red. Next, the Au seed solution was added to the mixture of  $\text{HAuCl}_4$  (165  $\mu\text{L}$ , 1% wt), 240  $\mu\text{L}$  of MSA (10 mM), and 20 mL of water. After stirred at room temperature for 2 h, the Au NPs solution was obtained.

## 3. Cell culture

Human breast cancer cells (MCF-7) and human cervical cancer cells (HeLa) were cultured in DMEM high glucose medium supplemented with 10% fetal bovine serum, 100 U/mL penicillin, and 100 mg/mL streptomycin at 37 °C in a 5%  $\text{CO}_2$  humidified atmosphere. The human breast normal cell line (MCF-10A) was cultured similarly but in RPMI 1640 medium instead of DMEM. During logarithmic growth, cells were digested with trypsin, suspended in a centrifuge tube, and then centrifuged at 750 rpm/min for 3 min. After removing the supernatant, the cells were resuspended in 2 mL of PBS buffer for subsequent experiments.

## 4. Cell number and capture efficiency

10  $\mu\text{L}$  of the above cell suspension was added to a hemocytometer for counting to estimate the number of cells in the culture flask. Based on the cell count, the suspension was diluted to various concentrations ( $1 \times 10^2$ ,  $5 \times 10^2$ ,  $1 \times 10^3$ ,  $5 \times 10^3$ ,  $1 \times 10^4$ ,  $5 \times 10^4$ ,  $1 \times 10^5$ ,  $5 \times 10^5$ ,  $1 \times 10^6$  cells/mL) and cultured on modified electrodes. The cells were stained with 0.5  $\mu\text{L}$  Calcein AM for 15 min and observed under a laser confocal microscope to count the number of cells ( $N_1$ ). The cell number ( $N_0$ ) under the determined concentration ( $C$ ) and volume ( $V$ , 50  $\mu\text{L}$ ) was calculated as  $N_0 = (S_1 / S_0) \times C \times V$ , in which  $S_0$  refers to the electrode area that defined by the 5 mm diameter hole in the insulating tape, and  $S_1$  refers to the actual measured area from the confocal microscopy images, analyzed using ImageJ software. And the cell capture efficiency ( $E$ ) was then calculated as  $E = (N_1 / N_0) \times 100\%$ .

## 5. Optimization of the cytosensor

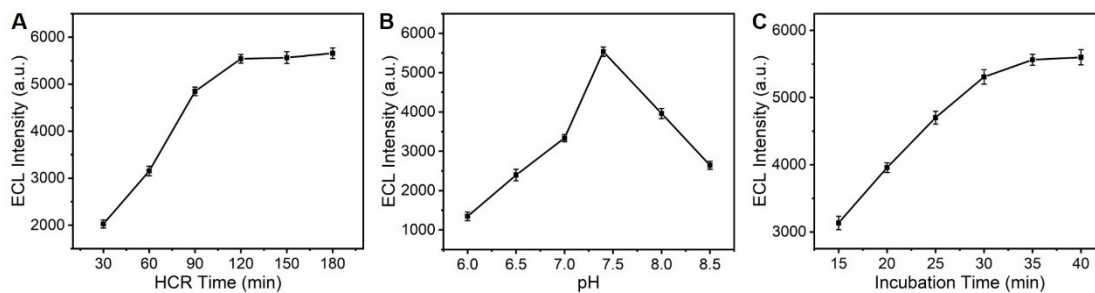


**Fig. S1.** Optimization of experimental conditions. Effects of (A) HCR time, (B) solution pH, and (C) incubation time of SA@Ru-M1 on ECL signal intensity.

## 6. Detection performance evaluation

The cell suspension volume used for capture and detection was 50  $\mu\text{L}$  ( $V$ ), and the optimal cell capture efficiency of the sensor interface was approximately 83.7% ( $E$ ). When the sample concentration is 31 cells/mL ( $C$ ), achieving the detection limitation, the theoretical number ( $N$ ) of cells captured on the electrode surface is estimated as  $N=C\times V\times E=50\times 31\times 83.7\%\times 10^{-3}=1.3$  cells. This indicates the potential of this cytosensor for single-cell level detection.

## 7. Comparison of different methods for CTCs detection

As shown in Table S2, existing CTC capture and detection methods exhibit distinct focuses in terms of nanostructured substrates, capture efficiency, and detection performance. Nanofiber substrates, known for their three-dimensional porous architecture and biomimetic topological features, are frequently employed for efficient cell capture. Their reported efficiencies typically range from 60% to 90%, and they often rely on fluorescence imaging for readout. Other nanomaterial-assisted platforms can achieve lower detection limits, yet often struggle to combine high capture performance with real-time sensing. In this work, the PANI nanofiber-based substrate not only delivers high capture efficiency (83.7%) but also integrates capture with ECL detection, enabling synchronous quantification across a broad range of  $10^2$ - $10^6$  cells/mL with a detection limit of 31 cells/mL, thereby offering an efficient and integrated sensing platform for CTC analysis.

**Table S2.** Comparison between the proposed cytosensor and other methods for detecting CTCs

Detection method/ capture mode	Nanostructured substrates	Capture efficiency	Biorecognition element	Detection range (cells/mL)	LOD (cells/ mL)	Ref.
FL imaging	Chitosan nanofibers	53.8-66.5%	pCBMA aptamer	20-200	/	[1]
FL imaging	PLGA nanofibers	>70%	anti-EpCAM	10-200	10	[2]
FL intensity	core-shell nanofibrous PCL membrane	75%	Hyaluronic acid	$5 \times 10^2$ - $5 \times 10^4$	/	[3]
FL imaging	PS-PSMA nanofibers	59-67%	anti-EpCAM	$1-1 \times 10^5$	/	[4]
Organic bioelectronic platform	PEDOT-based nanofiber	>90%	anti-EpCAM	$2 \times 10^6$ (500 $\mu$ L)	/	[5]
Organic electrochemical transistors	Coronene nanofiber arrays	>90%	anti-EpCAM	$1 \times 10^4$ - $1 \times 10^6$	/	[6]
microfluidic chip-SERS	PMMA-triangular column	86.87%	wy5a aptamer	/	/	[7]
Photoelectrochemical- FL imaging	DNA-linked CdTe QDs/Bi <sub>2</sub> MoO <sub>6</sub> /CdS	/	aptamer	$50-1 \times 10^5$	1	[8]
Electrochemistry	PVDF/CS	66%	anti-EpCAM	$1 \times 10^1$ ~ $1 \times 10^7$	10	[9]
ECL	$\beta$ -CD-AuNPs/graphene	/	aptamer	$50-1 \times 10^3$	40	[10]
ECL	hierarchical flower-like gold array	89%	MUC1 aptamer	$1 \times 10^2$ - $1 \times 10^6$	18	[11]
ECL	3D multivalent aptamer	88.7%	MUC1/ EpCAM- aptamer	$8 \sim 1 \times 10^5$	2	[12]
ECL	PANI nanofiber	83.7%	EpCAM- aptamer	$1 \times 10^2$ - $1 \times 10^6$	31	This work

## References

- [1] N. Sun, M. Liu, J. Wang, Z. Wang, X. Li, B. Jiang and R. Pei, *Small*, 2016, **12**, 5090-5097.
- [2] H. Liu, Z. Wang, C. Chen, P. Ding, N. Sun and R. Pei, *Colloids and Surfaces B: Biointerfaces*, 2019, **181**, 143-148.
- [3] S. Asghari and M. Mahmoudifard, *Journal of Biomededical Materials Research*, 2023, **111**, 1121-1132.
- [4] J. Yoon, H. S. Yoon, Y. Shin, S. Kim, Y. Ju, J. Kim and S. Chun, *Nanomedicine: Nanotechnology, Biology and Medicine*, 2017, **13**, 1617-1625.
- [5] C. Yu, B. C. Ho, R. S. Juang, Y. S. Hsiao, R. V. R. Naidu, C. W. Kuo, Y. W. You, J. J. Shyue, J. T. Fang and P. Chen, *ACS Appl. Mater. Interfaces*, 2017, **9**, 30329–30342.
- [6] L. Zhao, Y.T. Lu, F. Li, K. Wu, S. Hou, J. Yu, Q. Shen, D. Wu, M. Song, W.H. OuYang, Z. Luo, T. Lee, X. Fang, C. Shao, X. Xu, M.A. Garcia, L.W. Chung, M. Rettig, H.R. Tseng and E.M. Posadas, *Advanced Materials*, 2013, **25**, 2897-2902.
- [7] Y. Zhou, H. Cong, R. Gao, H. Zhu, Y. Liu, B. Li, Y. Feng and L. Yu, *Microchemical Journal*, 2025, **209**, 112613.
- [8] S. Duan, H. Zhang, Z.Liu, J. Li, L. Gao, H. Jiang and J. Wang, *Talanta*, 2025, **292**, 127922.
- [9] Y. Wu, Y. Wang, R. He, Y. Li and Y. Ben, *RSC Advances*, 2025, **15**, 32546-32552.
- [10] Q. Kun, Y. Lin, H. Peng, L. Cheng, H. Cui, N. Hong, J. Xiong and H. Fan, *Journal of Electroanalytical Chemistry*, 2018, **808**, 101-106.
- [11] M. Li, J. Shi, Y. Zhang, S. Cui, L. Zhang and Q. Shen, *Analytica Chimica Acta*, 2024, **1303**,342505.
- [12] M. Guo, B. Shen, W. He, X. Li, X. Li, M. Li, R. Hu, M. Zhang and Y. Yan, *Chemical Engineering Journal*, 2024, **481**,148606.